

Two old ways to measure the electron-neutrino mass

A. De Rújula

IFT(UAM), Madrid, Spain; CERN, 1211 Geneva 23, Switzerland

(Dated: June 2, 2022)

Three decades ago, the measurement of the electron neutrino mass in atomic electron capture (EC) experiments was scrutinized in its two variants: single EC and neutrino-less double EC. For certain isotopes an atomic resonance enormously enhances the expected decay rates. The favoured technique, based on calorimeters as opposed to spectrometers, has the advantage of greatly simplifying the theoretical analysis of the data. After an initial surge of measurements, the EC approach did not seem to be competitive. But very recently, there has been great progress on micro-calorimeters and the measurement of atomic mass differences. Meanwhile, the beta-decay neutrino-mass limits have improved by a factor of 15, and the difficulty of the experiments by the cube of that figure. Can the “calorimetric” EC theory cope with this increased challenge? I answer this question affirmatively. In so doing I briefly review the subject and extensively address some persistent misunderstandings of the underlying quantum physics.

Keywords: electron neutrino mass, electron capture, calorimetry, ^{163}Ho , ^{152}Gd .

I. MOTIVATION

In 1933 Perrin qualitatively described [1] and Fermi computed [2] how a nonzero neutrino mass would affect the endpoint of the electron energies in a β -decay process. Two score years later, the laboratory quest for a non-zero result in this kind of measurement continues in earnest [3].

In a 1980 paper with almost the same title as this one [4] I discussed the possibility to measure or constrain the mass of the electron neutrino in various processes involving electron capture (EC). This is the $ep \rightarrow \nu n$ weak-interaction process whereby an atomic electron interacts with a nucleus of charge Z to produce a neutrino, leaving behind a nucleus of charge $Z - 1$ and a hole in the orbital of the daughter atom from which the electron was captured. There we noted that –if nature was kind enough in choosing the relevant parameters of some isotopes– the endpoint counting rates would be significantly enhanced by atomic resonances and that “calorimetric” measurements would obviate the complications induced by “atomic and molecular problems”. EC would complement the classical approach [1, 2] employing nuclear β -decay –notably of ^3H (Tritium) and ^{187}Re – to constrain the mass of the electron “anti”-neutrino [3].

Several experiments were performed in the 1980’s to study the feasibility of the proposed method with the conclusion that EC was not competitive with ^3H β -decay, under the eminently reasonable assumption that the two mentioned distinct neutrinos have the same mass. Very recently, the hopes concerning electron-capture experiments have been rekindled, an opportunity to manifest glee for the experiments and to review and further complete the theory, which for a case of current interest: calorimetric measurement in the EC decay of ^{163}Ho , was first developed in detail in [5].

Calorimetry is also being pursued in the β -decay of ^{187}Re [7]. Here the theory, as we shall mention, is not as simple as for EC decays. One reason why substances as exotic ^3H , ^{187}Re and ^{163}Ho are employed is that the total

energy released in their decays –the Q -values– are the next to smallest or smallest of the periodic table, so that the fraction of m_ν -sensitive events is largest. Another reason is that their lifetimes are not prohibitively long.

Neutrino-less double β decay is the classic method to attempt to establish the Majorana or Dirac nature of massive neutrinos, while measuring a function of their masses. This process also has an EC analog: neutrino-less double electron capture [9–11]. There is also very significant progress concerning the prospects of calorimetry in this field, mainly involving the decay of ^{152}Gd [12].

Naturally, the ultimate goal of all the mentioned experiments, and others, is to compete with the current best laboratory limits on the electron antineutrino mass:

$$m_{\bar{\nu}} < 2.3 \text{ eV (95\% C.L.)}, \quad (1)$$

$$m_{\bar{\nu}} < 2.05 \text{ eV (95\% C.L.)}, \quad (2)$$

from the Mainz and Troitsk data, respectively [13, 14].

At the time the theories of resonant single [5] and double [11] EC were elaborated, the limits on –or alleged measurements of– $m_{\bar{\nu}}$ were at the 30 eV level. The relative yield of events sensitive to $m_{\bar{\nu}}$ or m_ν in a specific decay scales like m^3 , so that the experiments have in this sense become approximately $(30/2)^3 \sim 3.4 \times 10^3$ times more demanding. The question arises whether or not the underlying EC theory is precise enough to deal with the current experimental situation. The main aim of this paper is to answer this question –affirmatively– in the case of the EC and DEC current and planned campaigns.

II. A TRIVIAL REMINDER

Consider the β decay, $^3\hat{\text{H}} \rightarrow ^3\hat{\text{He}} e^- \bar{\nu}$, of a free Triton ($^3\hat{\text{H}} = ^3\text{H}^+$, $^3\hat{\text{He}} = ^3\text{He}^{++}$) and ignore radiative corrections, neutrino mixing and the (negligible) nuclear-recoil effect. Define $Q = M_i - M_f$, with i, f the initial and final nuclei. Let $F(E_e)$ be the “Fermi” function reflecting the fact that the electron is born in a Coulombic field. Let

\mathcal{M} be the $n \rightarrow p e \bar{\nu}$ matrix element and Φ the phase space factor. Very explicitly, the differential decay width is:

$$\frac{d\Gamma}{dE_e} = \frac{1}{2} |\mathcal{M}|^2 F(E_e) \Phi, \quad (3)$$

$$|\mathcal{M}|^2 \approx 32 G_F^2 \cos^2 \theta_C M_i M_f (1 + 3 g_A^2) E_e E_{\bar{\nu}}, \quad (4)$$

$$\Phi = \frac{1}{8 \pi^3} \frac{p_e p_{\bar{\nu}}}{M_i M_f}, \quad (5)$$

$$p_{\bar{\nu}} = \sqrt{E_{\bar{\nu}}^2 - m_{\bar{\nu}}^2}, \quad E_{\bar{\nu}} = Q - E_e, \quad (6)$$

where $g_A \approx 1.23$ is the nucleon axial coupling. In Eq.(4), $|\mathcal{M}|^2$ takes into account that $\{^3\hat{H}, ^3\hat{He}\}$ is an isospin doublet (misaligned" by $\approx \cos \theta_C$ with a weak isodoublet) so that the Fermi matrix element $\langle ^3\hat{He} | \sum_1^3 \tau_i^+ | ^3\hat{H} \rangle$ is unity. Similarly, given the simple structure of these nuclei, the Gamow-Teller matrix element is $|\langle ^3\hat{He} | \sum_1^3 \tau_i^+ \vec{\sigma}_i | ^3\hat{H} \rangle| \simeq \sqrt{3}$, exact for a free neutron [15].

We know from the observations of neutrino oscillations that the electron neutrino is, to a good approximation, a superposition of three mass eigenstates, ν_i : $\nu_e = \sum_i U_{ei} \nu_i$, with $\sum_i |U_{ei}|^2 = 1$. Thus, we ought to have written $d\Gamma/dE_e$ in Eq. (3) as an incoherent superposition of spectra with weights $|U_{ei}|^2$ and masses $m(\nu_i)$. But the measured differences $m^2(\nu_i) - m^2(\nu_j)$ are so small that current direct attempts to measure the quantity $m_{\bar{\nu}}$ of Eq. (6) are certain to reach the required accuracy only if neutrinos are nearly degenerate in mass, in which case m_{ν} in Eqs. (3-6) stands for their nearly common mass.

The function on which the ‘‘Kurie plots’’ are based is:

$$\begin{aligned} K(E_e) &\equiv \sqrt{\frac{d\Gamma}{F(E_e) p_e E_e dE_e}} \propto \sqrt{E_{\bar{\nu}} p_{\bar{\nu}}} \\ &= \sqrt{(Q - E_e) \sqrt{(Q - E_e)^2 - m_{\bar{\nu}}^2}}, \end{aligned}$$

a straight line ending at $E_e = Q$ if $m_{\bar{\nu}} = 0$. The spectrum near the endpoint for $m_{\bar{\nu}} = 0$ is quadratic in $Q - E_e$. The fraction of events potentially sensitive to $m_{\bar{\nu}} \neq 0$ – in an interval of width of $\mathcal{O}(m_{\bar{\nu}})$ – scales as $m_{\bar{\nu}}^3$, and so do the challenges to experiment and theory.

The neutrino-mass sensitive factor $p_{\bar{\nu}}$ in $K(E_e)$ arises exclusively from phase space, it depends on the mass difference Q but is otherwise independent of the constituency of the nuclei considered. Going one step inwards in ‘‘resolution’’, the description of the $p e \bar{\nu}$ decay of a free neutron is independent of the nucleons’ constituent quarks and gluons, but for the fact that they determine (in principle) m_n , m_p and g_A .

The laboratory constraints on $m_{\bar{\nu}}$ from ^3H decay have continued to improve quite impressively in the past two decades, as summarized in Fig. (1), from [3]. The current endeavours are not trifling, as illustrated in Fig. (2), depicting a toilsome moment in the transport of KATRIN’s spectrometer to Karlsruhe, after a 9000 km journey through the Danube, the Black Sea, the Mediterranean, the Atlantic, the North Sea and the Rhine [3].

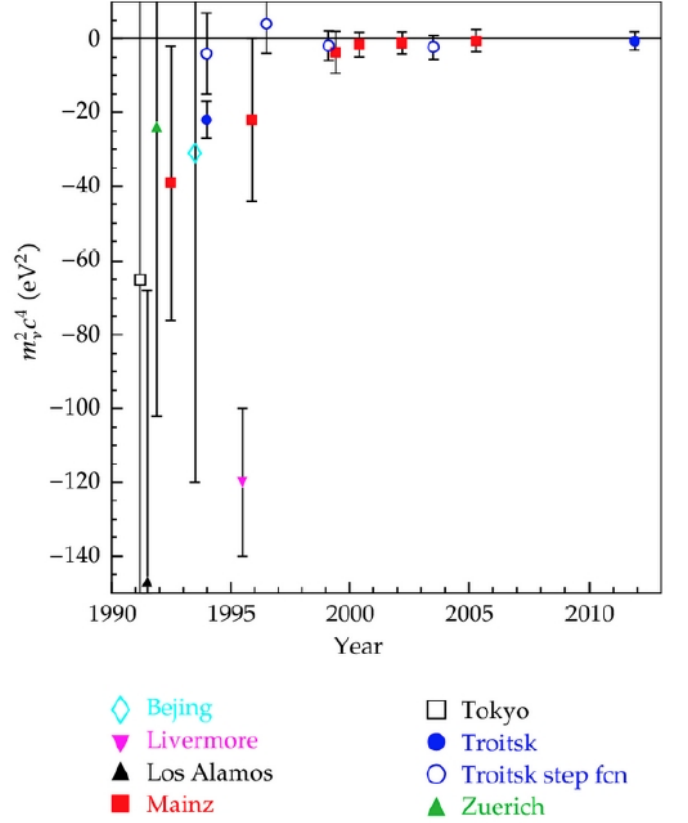


FIG. 1: Relatively recent progress and some errors in constraining $m_{\bar{\nu}}$ from ^3H β -decay, as summarized in [3].



FIG. 2: The spectrometer of KATRIN in dire straits.

Across the Atlantic there is an ongoing test [17] of the novel idea behind Project 8: to measure single electron energies via their coherent synchrotron radiation [18].

III. THE CALORIMETRIC ‘‘PRINCIPLE’’

A calorimeter, in our discussion, is a detector in which the decaying source is embedded, capable of measuring

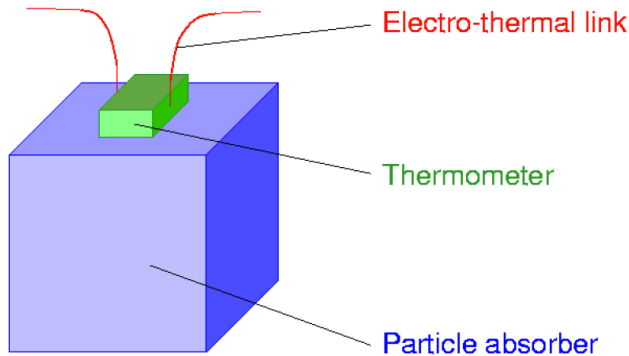


FIG. 3: A theorist's calorimeter [3]. The source is implanted in the absorber, where all energy but that of escaping neutrinos is deposited and measured as a rise of temperature.

all the energy released in a weak decay, but that of the escaping neutrino. A view of a calorimeter, presumably meant for theorists, is shown in Fig. 3.

Somewhat reminiscent of the Mössbauer effect, the calorimetric “principle” follows from the realization that one can extend the phase-space considerations of §II outwards in resolution, from quarks, nucleons and nuclei all the way to the decay of the detector before to the detector after the neutrino (and nothing else) escaped from it. Calling $D_{b,a}$ the detector before and after, and E_c the measured calorimetric energy, the overall process, $D_b \rightarrow D_a + E_c + E_\nu$, is a three-body decay with kinematics –and consequent neutrino-mass sensitivity– as simple as the ones of neutron decay, with Q being now defined as $m(D_a) - m(D_b)$.

A problem that has traditionally pestered ^3H experiments (almost all of which were non-calorimetric) is that the final atom or molecule may be left in excited states of energy E_n above the ground state. In a β -decay experiment in which the electron energy is measured, energy conservation implies $Q = E_e + E_{\bar{\nu}} + E_n$, so that the electron spectrum is a superposition of contributions whose end-points are at $E_e = Q - E_n - m_{\bar{\nu}}$. The spectral shape from which $m_{\bar{\nu}}$ is to be inferred is a complicated superposition of spectra with different endpoints. This is the well known “atomic or molecular” problem.

The main advantage of a calorimeter is that its measurements are independent of the various states in which a daughter atom, molecule or crystal may be left, as well as the various decay channels (X -rays or electron-emitting transitions) via which the excited final states return to the ground state. If the de-excitation times, as expected, are much shorter than the signal's rise-time all de-excitation energies of a decay event add up in E_c .

The main disadvantage of a calorimeter is that –unlike in a β -decay spectrometer– there is no way to veto events whose energy is well below the interesting end-point region. The full E_c spectrum is measured. To avoid pile-up (simultaneously measured events), the activity

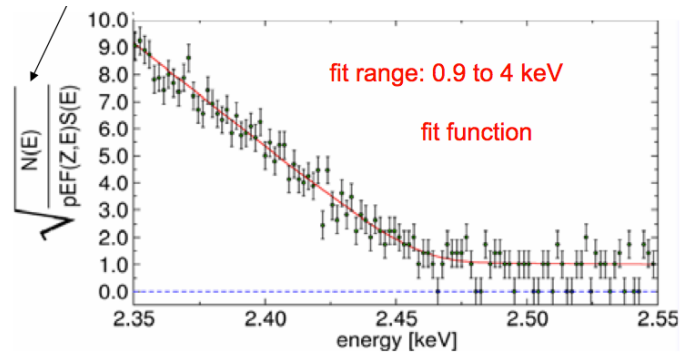


FIG. 4: A ^{187}Re Kurie plot from MIBETA [7].

of the source/detector must be limited. This means that “calorimeter farms” with up to thousands of micro-calorimeters must be contemplated. But their individual elements are minute: barely visible to the naked eye!

Strictly speaking, the calorimeter considerations we have discussed apply only to allowed weak decays, of which the ^3H and ^{163}Ho cases are examples. For them the nontrivial nuclear-dependence of the matrix element $|\mathcal{M}|^2$ is just a number, $1 + 3g_A^2$ in n or ^3H decay. In a forbidden decay such as that of ^{187}Re , the outgoing e^- or $\bar{\nu}$ must carry away angular momentum, which induces an E_e -dependence of the corresponding $|\mathcal{M}|^2$. Though not to leading order, this reintroduces the need to deal with the different atomic or molecular excitations [16].

IV. ^{187}Re AND ^{163}Ho EXPERIMENTS

The ground-state to ground-state nuclear transition $^{187}\text{Re}(5/2)^+ \rightarrow ^{187}\text{Os}(1/2)^-$ has a record-low $Q \simeq 2.47$ keV and is “first unique forbidden”. Consequently the half-life of ^{187}Re is long: $4.3 \cdot 10^{10}$ years, comparable to the current age of the Universe. Two groups have been pursuing measurements with ^{187}Re -implanted calorimeters: MANU [8] and MIBETA [7]. Their published limits are, respectively:

$$\begin{aligned} m_\nu &< 26 \text{ eV at } 95\% \text{ CL}, \\ m_\nu &< 15.6 \text{ eV at } 90\% \text{ CL}. \end{aligned} \quad (7)$$

A MIBETA Kurie plot is shown in Fig. 4.

The decay $^{163}\text{Ho}(7/2)^- \rightarrow ^{163}\text{Dy}(5/2)^-$ is an allowed ground-state to ground-state nuclear transition. Its half-life is a mere ~ 4.6 millennia. A Q -value of 2.80 ± 0.08 keV, recently obtained with a prototype calorimeter [19], disagrees with the “recommended” (and often unadvisable) $Q = 2.555 \pm 0.016$ keV [20]. For neutrino mass measurements it is in all cases foreseen and truly commendable to determine the Q -values independently and very precisely with use of Penning trap techniques, which have recently improved dramatically [21].

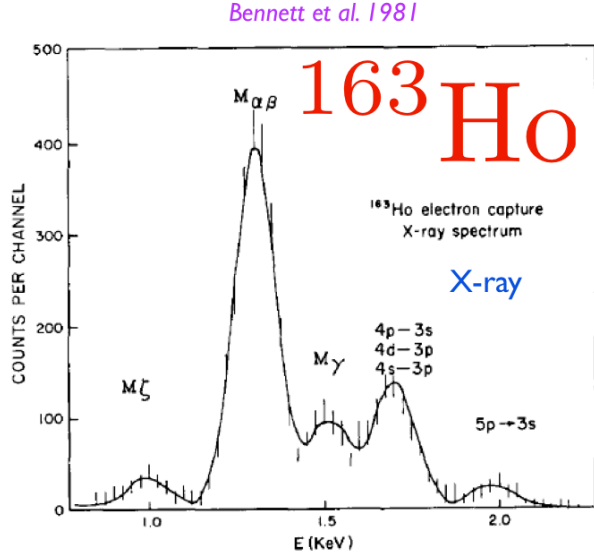


FIG. 5: IBEC spectrum in ^{163}Ho decay [22], showing prominent X-ray lines.

Some early measurements with a ^{163}Ho source [22, 23] were based on IBEC (Internal Bremsstrahlung in Electron Capture), the first-principle theory of which is fiendishly complex both above [24] and –more so– below [4] the energies coinciding with X-ray resonances. One example is shown in Fig. 5. Other measurements were calorimetric [25], see Fig. 6. The most stringent of the early mass limits, from [23] and [26] were, respectively:

$$\begin{aligned} m_\nu &< 225 \text{ eV at 95\% CL,} \\ m_\nu &< 490 \text{ eV at 68\% CL.} \end{aligned} \quad (8)$$

The recent progress may be illustrated by comparing Fig. 6 [25] with the preliminary results shown in Fig. 7, from the incipient experiment ECHo [27], which employs MMCs (Magnetic Metallic Calorimeters). The unlabeled peaks in Fig. 7 are due to ^{144}Pm , an impurity accompanying ^{163}Ho at the implantation stage at ISOLDE-CERN, an early test of source-preparation techniques.

One cannot resist the temptation of showing a scheme and a picture of the set of four MMCs in the ^{163}Ho detector prototype of ECHo [27]: Figs. 8 and 9. There is satisfaction associated with the possibility of measuring a tiny quantity –the neutrino mass– with nano-scale detectors. Even with the associated cryogenics and electronics, the apparatuses are still table-top.

V. THE THEORY OF EC IN ^{163}Ho

The EC process, all by itself, does not yield any information on the neutrino mass, or on anything else, for that matter. The mere information that “it happened” is

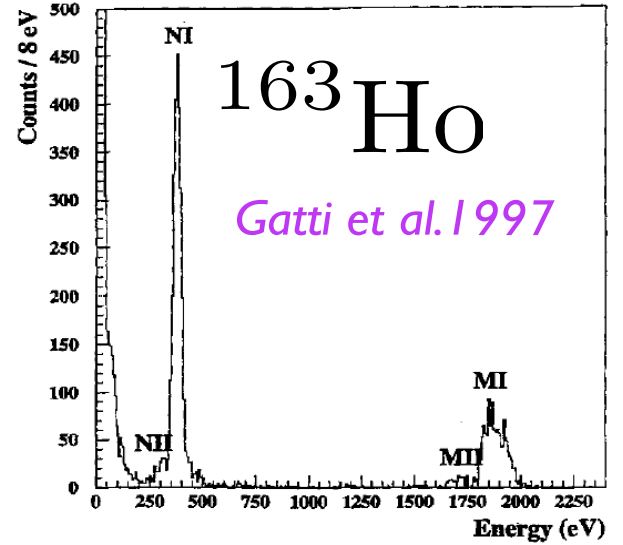


FIG. 6: Results of an early ^{163}Ho calorimetric spectrum [25].

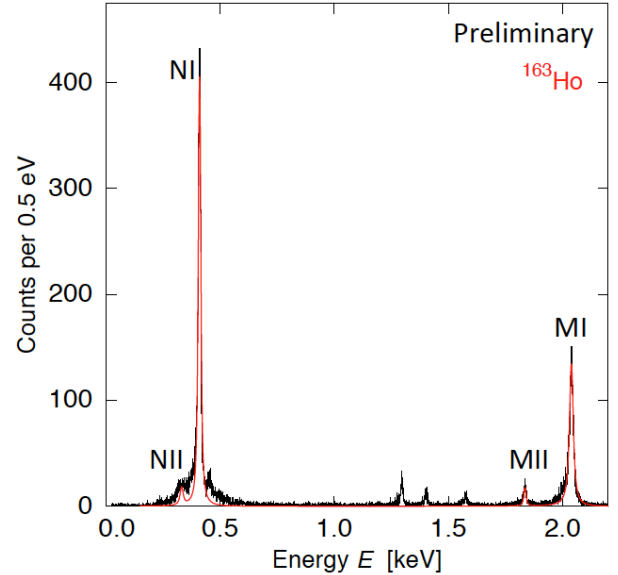


FIG. 7: Test results of ECHo [27] for the calorimetric spectrum of ^{163}Ho decay. The unlabeled impurities are ^{144}Pm . The continuous (red line) theory [5] is based on Eq. (9).

provided by the fact that the daughter atom, and sometimes its nucleus, are unstable. The hole in an atomic shell, for instance, results in observable X-rays, as the outer electrons cascade inwards, see Fig. 5.

The measured $Q = M(^{163}\text{Ho}) - M(^{163}\text{Dy})$ is so small that EC is only energetically allowed from ^{163}Ho orbitals with principal quantum number $n > 2$. The emission of X-rays from holes in such external shells is negligible compared to that of atomic de-excitations involving electron emission (in the classical parlance, the “fluorescence yields” are tiny). The electron-emitting transitions have

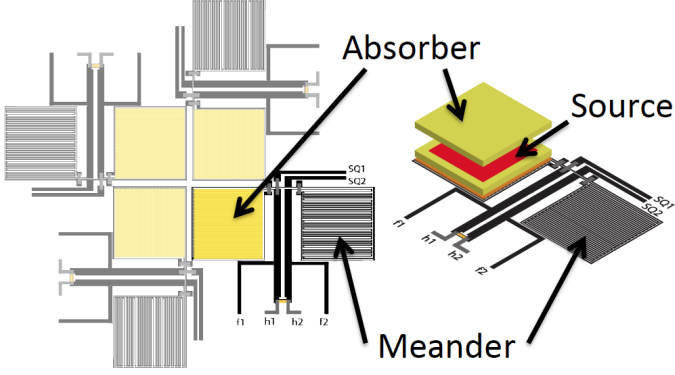


FIG. 8: Schematic view of an ECHO prototype. The temperature change following a ^{163}Ho -decay event which deposits an energy E_c in a gold absorber is measured by the change of magnetization of a paramagnetic sensor material (Au:Er). The “meanders” are coupled superconducting Nb pickup coils.

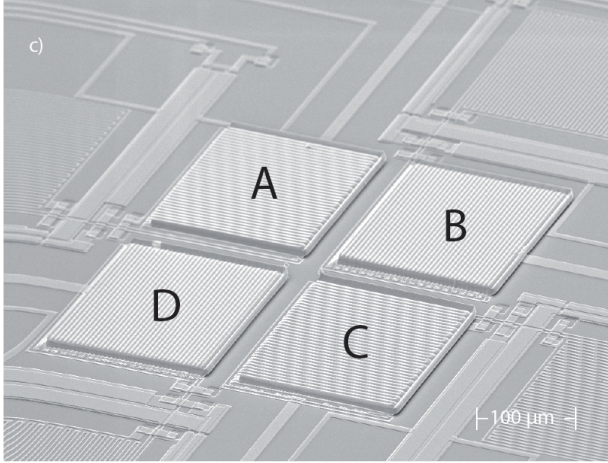


FIG. 9: ECHO prototype micrograph. Notice the scale, implying that the hole picture’s surface is $\mathcal{O}(1) \text{ mm}^2$.

more names than interest, depending on whether or not the involved electron orbitals have the same or different n . This is illustrated, for the sake of history, in Fig. 10.

Let $\{n, l_j\}$ denote an atomic orbital with principal quantum number n , and orbital (total) angular momentum $l(j)$. To keep its language obsolete, atomic physics still refers to $n = 1, 2, 3, 4, \dots$ as K, L, M, N..., to $\{n, l\} = \{1, 0\}, \{2, 0\}, \{3, 0\}, \{4, 0\}, \dots$ as K1, L1, M1, N1..., to $\{n, l\} = \{1, 1\}, \{2, 1\}, \{3, 1\}, \{4, 1\}, \dots$ as K2, L2, M2, N2..., and to $l = 0, 1, 2, \dots$ as S, P, D,...

For an atomic electron to be captured by its nucleus, it must be that its wave function at the origin, $\varphi(0)$, be

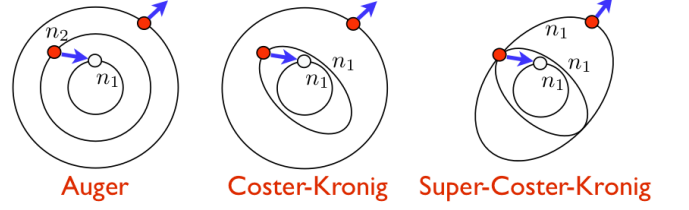


FIG. 10: The names of electron-ejection de-excitations. The holes left by EC are the hollow circles. The n_i are principal quantum numbers, which in the right-most figure all coincide.

non-vanishing, as is the case for the angular momentum $l = 0$, $n = 3, 4, 5$ and 6 shells M1, N1, O1 and P1 in ^{163}Ho . Capture from $nP_{1/2}$ shells is forbidden in a non-relativistic approximation, since $\varphi(0) = 0$ for $l \neq 0$. But the spin-orbit coupling induces an opposite orbital parity $nS_{1/2}$ admixture of order αZ in the “small” components of the electron wave function, from which the electron can be captured. Total angular momentum conservation forbids capture from $nP_{j \geq 3/2}$ but for tiny corrections arising from the finite nuclear size.

All in all, in ^{163}Ho , energy and angular-momentum conservation allow EC from the orbitals M1, M2, N1, N2, O1, O2 and P1, above which Ho runs out of electrons.

We argued in [5] that the matrix element for electron capture in ^{163}Ho may be very well approximated in an “effective” theory extraordinarily simpler than a first-principle QED approach [4]. The trick consists, as in the Fig. 11, in viewing the process as a two-step one. First a two-body decay $^{163}\text{Ho} \rightarrow ^{163}\text{Dy}^H + \nu_e$, with Dy^H any of the relevant daughter states with a hole in the orbital H. Second, the de-excitation $^{163}\text{Dy}^H \rightarrow ^{163}\text{Dy} + E_c$, the details of which need not be specified. The double steps are to be summed over holes. Ignoring for the moment a series of complications that we shall prove to be irrelevant, the differential decay rate is then:

$$\begin{aligned} \frac{d\Gamma}{dE_c} &\propto (Q - E_c) \sqrt{(Q - E_c)^2 - m_\nu^2} \\ &\quad * \sum_H \varphi_H^2(0) B_H \frac{\Gamma_H}{2\pi} \frac{1}{(E_c - E_H)^2 + \Gamma_H^2/4} \\ &\implies \mathcal{K} (Q - E_c) \sqrt{(Q - E_c)^2 - m_\nu^2}, \end{aligned} \quad (9)$$

where $B_H - 1$ [6] is an $\mathcal{O}(10\%)$ correction for atomic exchange and overlap. The contributions to the sum in Eq. (9) have a common endpoint at $E_c = Q - m_\nu$ for all H, with \mathcal{K} (describing the spectrum near to its endpoint), a constant to a level of precision to be discussed anon.

It is laborious to precisely compute from first principles the atomic parameters appearing in Eq. (9). Trusting such a calculation one may use its form, convoluted with the experimental resolution, to obtain information

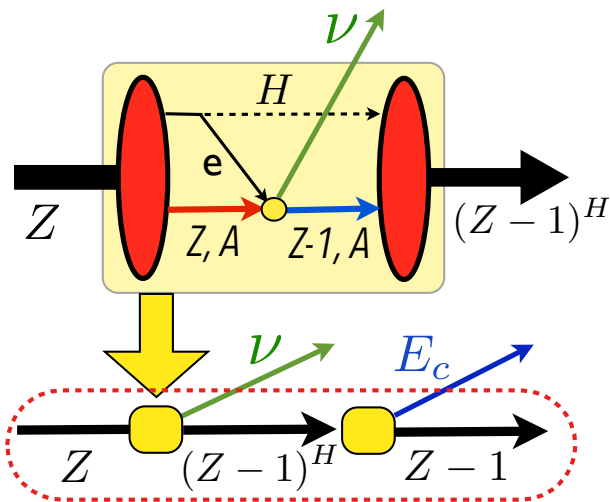


FIG. 11: Effective theory of electron capture [5]. The upper capsule embodies the details for the decay into a daughter atom with an electron hole H . The lower (dashed) capsule also incorporates the transition to the detector's final ground state. The calorimetric energy E_c is not meant to escape, but to be converted into a deposited-energy signal.

on Q and even m_ν . In practice it may be best to use an independently determined Q [21], and to fit the data to the observed widths and spectral peak ratios to extract, respectively, Γ_H and the ratios of the quantities $\varphi_H^2(0) B_H \Gamma_H$. While this may be useful in providing a fair fit to the full spectral data, it is immaterial to the extraction information on m_ν from the endpoint spectral domain. There, as we shall see, the resonance-dominated atomic matrix element is practically constant.

A recent result based on Eq. (9) is shown in Fig. 12 [28], for $Q = 2.5$ keV, $B_H = 1$, E_H and Γ_H as in [29] and the ratios $\varphi_H^2(0)/\varphi_{M1}^2(0)$ as tabulated in [30].

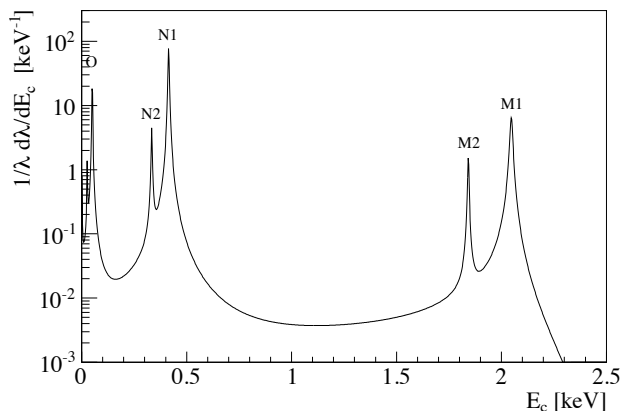


FIG. 12: The calorimetric spectrum of ^{163}Ho decay [5, 28].

A. Complications?

1. The matrix element close to the endpoint

An important question is the range of the largest E_c values for which \mathcal{K} in Eq. (9) may in practice be taken to be a constant. The answer depends a bit on the ^{163}Ho decay Q -value, still insufficiently well measured. Consider the example $Q = 2.55$ keV and recall that $E_H \approx 2.05$ keV for $H = \text{M1}$ Dysprosium, the state of closest energy to the endpoint. In Fig. 13 we have plotted the phase-space factor of Eq. (9) for $m_\nu = 0$ and $m_\nu = 2$ eV, as well as the squared atomic matrix element (the sum over holes in the same equation), whose variation near the endpoint is essentially that of the function $1/(E_c - E[\text{M1}])^2$. All curves are normalized at the lowest E_c in the plot.

The point that Fig. 13 conveys is that the variation of the matrix element, simplified or not, is governed by atomic singularities located at the electron binding energies in Dy, as dictated by arguments as general as causality and analyticity. The precise absolute value of the matrix element may be hard to compute, but its variation cannot be large enough to be relevant in practice, unless the Q value happened to fall within a few widths of a resonance. Otherwise, the figure speaks for itself.

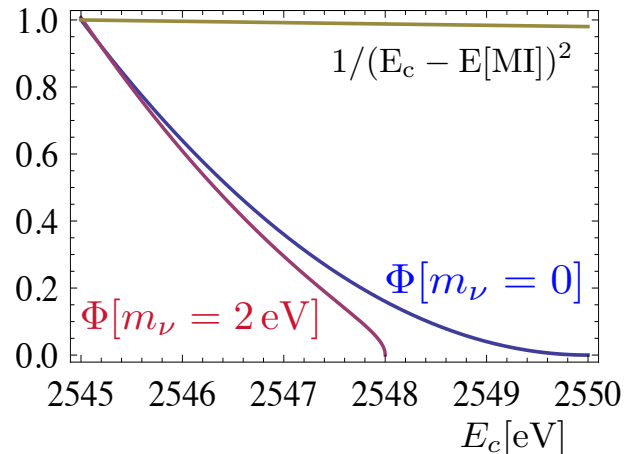


FIG. 13: Shapes at the endpoint of the $d\Gamma/dE_c$ spectrum in Ho decay, with an assumed $Q = 2.55$ keV. The $\Phi[m_\nu]$ lines are the phase-space function for two choices of m_ν . The line above them reflects the amount of energy-dependence expected for the squared matrix element. All curves are normalized to unity at the lowest E_c in the figure.

2. Quantum and classical effects

The expression Eq. (9) is “classical” in two respects: it does not contain “off-shell” intermediate states (the K and L, $n = 1$ and 2 virtual holes) and it is a sum of squared amplitudes and not an amplitude-sum squared.

The K and L summands are suppressed by large energy denominators and their negligible contribution has a squared matrix element at the endpoint that is even flatter in energy than the one illustrated in Fig. 13.

The neglected interferences must be small, as discussed in detail in [5], because the dominant decay channels for Dy with different electronic holes are different and consequently de-cohering. The dominant de-excitations of $H = nS, nP_{1/2}, n > 2$ states are Coster-Kronig transitions, $H \rightarrow H_1 H_2 e$, with one of the final holes in an orbital with the same original n , e.g. $\Gamma(\text{Coster-Kronig})/\Gamma(\text{Auger}) \simeq 16.6, 8.6, 166, 129$ for $H = M1, M2, N1, N2$, respectively [31]. In [5] we used the transition matrix elements of [31] to estimate that the effect of interferences is at most at the level of 1% towards the endpoint, and totally negligible in affecting its shape.

The neglected interferences ought to be most significant “half-way” between two neighboring resonances in the spectrum, far from the endpoint. A rough phenomenological way to deal with them and with non-resonant contributions (complementary to doing a commendable and precise atomic calculation) is to fit the data with two distinct widths per resonance: one below and one above the peak. Once more, for the extraction of information on m_ν , none of this would matter.

3. “Instantaneous” electron ejection

It may happen that the initial EC “instantaneously” leaves two holes in the daughter atom, because of the mismatch of the atomic orbitals before and after the capture. At first sight Eq. (9) does not include this direct manner of production of a final state with two vacancies (H_1 and H_2) in the daughter Dy atom:

$$\text{Ho} \rightarrow \text{Dy}[H_1, H_2] + e^- + \nu, \quad (10)$$

a three-body decay with the customary extended phase space for the distribution of electron energies.

The previous paragraph contains a “quantum misconception”. The “classical” instantaneous interpretation of Eq. (10) given in the previous paragraph is quantum-mechanically indistinguishable with another classical interpretation of the same process. To wit: electron capture leaving a hole in an orbital H , followed by an Auger or Coster-Kronig transition in which the hole migrates to H_2 and an electron is ejected, leaving an H_1 hole. The two classical interpretations refer to the same initial and final states: they are quantum-mechanically indistinct.

As an example, consider $H = M1, H_2 = M2, H_1 = N1$. This later process is resonant in that the ejected electron spectrum peaks at the mass difference between $\text{Dy}[M1]$ and $\text{Dy}[M2, N1]$ and the total calorimetric energy peaks at the Ho - Dy[M1] mass difference. But the process is one of the contributions to the $H = M1$ peak of Eq. (9). As for all processes, its contribution to the calorimetric energy spectrum extends all the way to its endpoint at $Q - m_\nu$, as dictated by mere energy conservation.

The extremely careful reader has noticed that there is one and only one potentially relevant process not subject to the two-fold classical interpretation we just discussed: the instantaneous decay

$$\text{Ho} \rightarrow \text{Dy}^{M1, N1} + e^- + \nu. \quad (11)$$

This decay is possible thanks to the slightly incomplete overlap between the wave function of the N1 electron in Ho and in Dy with an M1 vacancy. The charge that the N1 electrons feel in these two atoms is not the same, since electron screening is not perfect: as “seen” by an N1 electron, the M1 electron absent in the daughter dysprosium does not completely compensate for the absence of a proton in the Dy nucleus, relative to Ho.

The decay channel of Eq. (11) is non-resonant and has a negligible rate relative to the resonant processes described by Eq. (9). Moreover, the shape of its calorimetric endpoint is, once again, that of the last line of Eq. (9). It is instructive to prove these two points in some detail.

To get a very rough order of magnitude of the probabilities P_s for an N1 electron staying in place –and P_e for one of the two N1 electrons being instantaneously ejected– in the capture of an M1 electron, one may use Coulomb wave functions to get:

$$P_s = |\langle \Psi_{N1}(Z) | \Psi_{N1}(Z-1) \rangle|^2 = 1 - \frac{33}{4Z^2} + \mathcal{O}\left[\frac{1}{Z}\right]^3, \\ P_e \approx 2(1 - P_s) \approx \frac{33}{2Z^2} \approx 3.6 \times 10^{-3}, \text{ for } Z = 68. \quad (12)$$

A better estimate of P_e would be obtained with use of explicitly computed Ho and Dy atomic wave functions, but that would be an overestimate since the charge seen by the Dy N1 electrons is not $Z - 1$. Since there are no computed, readily available wave functions for Dy with an M1 hole, we shall evaluate all effects of screening.

A Coulomb wave function for M1 or N1 electrons with $Z = 68$ is also not a good choice since, again, it does not reflect the charge screening from the rest of the electrons, particularly the $n = 1, 2$ inner ones. To correct for this as we did in similar calculations in [32], let us introduce a Coulombic $Z_{\text{eff}}(n)$ giving the same mean orbital radii as in an elaborate calculation with Roothaan-Hartree-Fock atomic wave functions [33]. The results are:

$$Z_{\text{eff}}^{\text{Ho}}(M1) \approx 54.91, \quad Z_{\text{eff}}^{\text{Ho}}(N1) \approx 43.22, \\ Z_{\text{eff}}^{\text{Dy}}(M1) \approx 53.95, \quad Z_{\text{eff}}^{\text{Dy}}(N1) \approx 42.42. \quad (13)$$

From the Coulombic charge distributions, we can make an estimate of the charge, α , by which an M1 hole in Ho EC would screen an N1 electron in the daughter Dy:

$$\alpha = \int_0^\infty dr^3 \int_r^\infty dr'^3 |\Psi_{M1}(Z_{\text{eff}}^{\text{Ho}}(M1), r)|^2 |\Psi_{N1}(Z_{\text{eff}}^{\text{Dy}}(N1), r')|^2 \\ \approx 0.9649, \quad (14)$$

indicating a very large screening, i.e. $\epsilon \equiv 1 - \alpha \ll 1$. The use of Hartree-Fock wave functions, as opposed to

Z_{eff} approximations, gives results for quantities involving wave function overlaps, such as ϵ , that differ by no more than a factor of $\mathcal{O}(1)$ [32]. The advantage of the Coulombic approximation is that it makes the underlying physics very transparent, as in the next paragraph.

Define $\tilde{Z} \equiv Z_{\text{eff}}^{\text{Ho}}(N1)$ to write the probabilities introduced prior to Eq. (12), now fully corrected for screening:

$$\begin{aligned} P_s &= |\Psi_{N1}(\tilde{Z})\Psi_{N1}(\tilde{Z} - \epsilon)|^2 \\ &= 1 - \frac{33\epsilon^2}{4\tilde{Z}^2} \left\{ 1 + \mathcal{O}\left[\epsilon, 1/\tilde{Z}\right] \right\}, \\ P_e &\simeq 2(1 - P_s) \approx \frac{33\epsilon^2}{2\tilde{Z}^2} = 1.08 \times 10^{-5}. \end{aligned} \quad (15)$$

There is a slight enhancement relative to the naive estimate of P_e in Eq. (12), due to the change $Z \rightarrow \tilde{Z}$, and an enormous reduction due to the factor $\epsilon^2 \simeq 1.2 \times 10^{-3}$.

The conclusion is that the instantaneous decay of Eq. (11) is totally negligible ($P_e \ll 1$), relative to the M1 capture contribution to Eq. (9). Moreover, the shape of the corresponding squared matrix element close to the endpoint is the same as in that equation, since the extra factor p_e of electron-ejection phase space is compensated by the Fermi function $F(E_e)$, mentioned in § II, which at the relevant very low electron energies behaves as $1/p_e$. The atomic matrix element for the negligible process of Eq. (11) contains a non-resonant denominator $E_e + E(N1)$ that would have an even lesser shaping effect than the one illustrated in Fig. 13. Naturally, all this discussion ought to be complemented by an analogous one with $M1 \leftrightarrow N1$, the results of which are equally negligible.

4. Two experimental issues

Implicit in the calorimetric considerations of § III is the hypothesis that the de-excitation time of $^{163}\text{Dy}^{\text{H}}$ to its ground state is faster than the $\sim 0.1 \mu\text{s}$ rise-time for signals already achieved in prototype MMCs [34] (the signal decay-time is much longer). Atomic excited states having inverse widths of $\mathcal{O}(1) \text{ eV}^{-1} \sim 10^{-15} \text{ s}$, this seems to be a safe expectation, barring the existence of unforeseen metastable final states.

A more serious consideration is the possibility that Ho atoms in the detector be bound, not to one type of chemical neighbourhood, but to more than one. That would mean that the calorimeter is a sum of detectors with Q -values that may differ by an eventually significant amount [35].

VI. DOUBLE ELECTRON CAPTURE

Neutrino-less double β -decay has an EC analog: neutrino-less double electron capture [11]. The Feynman diagrams for double EC (DEC) processes, with two or no outgoing neutrinos, are shown in Fig. 14.

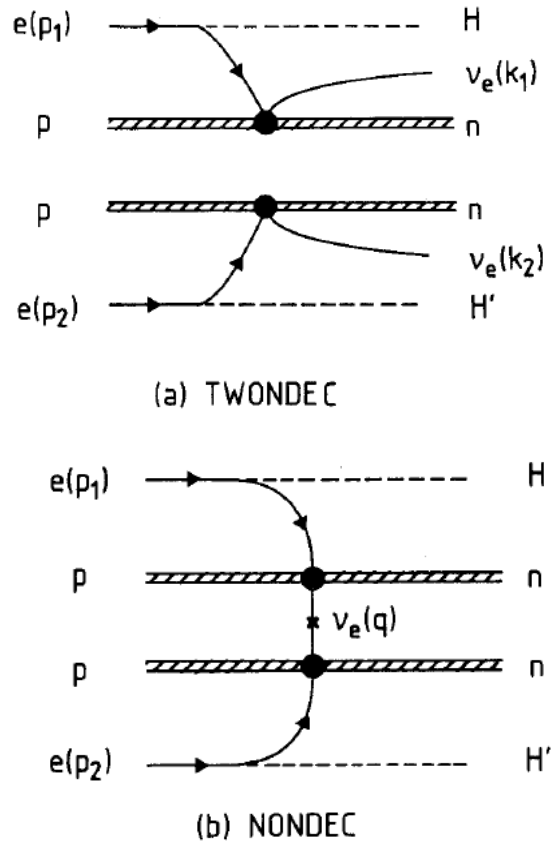


FIG. 14: Feynman diagrams for: (a) Two-neutrino double EC (TWONDEC). (b) No neutrino double EC (NONDEC) [11].

The level structure and energetics of the atoms that undergo DEC are illustrated in Fig. (15). An “intermediate” atom of nuclear charge $Z - 1$ β -decays to Z with a Q -value Q_β , and EC-decays to $Z - 2$ with a Q -value Q_{EC} . The mass difference between the ground-states of Z and $Z - 2$ is $Q = Q_{\text{EC}} - Q_\beta$. DEC from Z to $Z - 2$ is energetically allowed if Q is greater than the sum $E_H + E_{H'}$ of binding energies of the electron orbitals vacated by the double capture. The figure includes the possibility that the transition $Z \rightarrow Z - 2$ be to an excited daughter nucleus of energy E^* above the ground state. In that case, requiring $Q > E_H + E_{H'} + E^*$, the decay $(Z - 2)^* \rightarrow Z - 2 + \gamma$ may constitute an additional signature: the nuclear γ -ray.

Double β -decay experiments measure the spectrum of the sum of energies, E_T , of the two outgoing electrons. The dominant process has two outgoing neutrinos. The searched-for neutrino-less process would appear as a narrow peak, of width compatible with the resolution, at the endpoint of the E_T spectrum. The two-neutrino decay constitutes a significant irreducible background.

A potential advantage of neutrino-less DEC is that its corresponding two-neutrino irreducible background is, relative to the signal, rendered negligible by the three-body phase-space suppression of the background. A

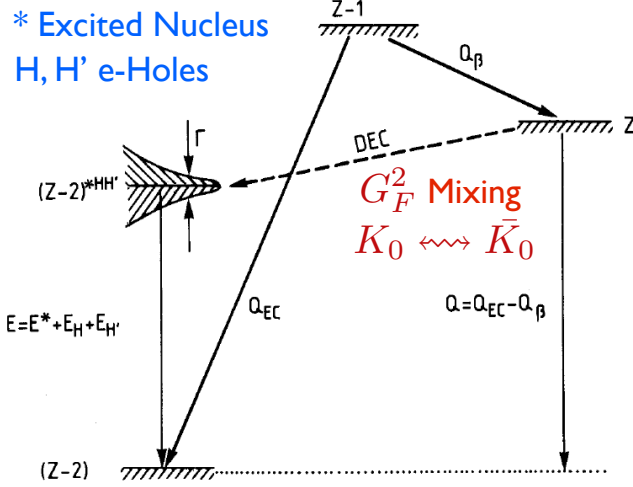


FIG. 15: Level structure of allowed DEC. The symbols and the analogy with $K^0 \leftrightarrow \bar{K}^0$ mixing are explained in the text.

calorimetric measurement would only see the peak at $E = E_H + E_{H'}$, if the daughter nucleus is stable. Otherwise, with a nuclear γ -ray also involved, one can think of many other possibilities, at least if “one” is a theorist.

A. The theory on neutrino-less DEC

In [11] we studied in detail neutrino-less DEC and the cases for which, in analogy with EC in ^{163}Ho , the process could be very significantly resonant-enhanced. At the time, the available information on the relevant Q -values was not very precise, and of the dozen nuclides we selected, $^{152}\text{Gd} \rightarrow ^{152}\text{Sm}$, a $0^+ \rightarrow 0^+$ (ground-state) nuclear transition, now appears to be an optimal candidate [21]. To wet the reader’s appetite for a reminder of the underlying theory, I show in Fig. 16 the resonant-enhancement factors for various DEC isotopes [21], normalized to the quintessential DEC-decaying one, ^{54}Fe . Most known relevant DEC cases are double-K orbital captures, an exception being the double-L capture in $^{164}\text{Er} \rightarrow ^{164}\text{Dy}$, also shown in the figure.

The neutrino mass parameter \bar{m}_ν relevant to neutrino-less DEC or double β -decay are obviously the same:

$$\bar{m}_\nu = \sum_i (U_{ei}^*)^2 m_i. \quad (16)$$

The theory of no-neutrino DEC can be easily understood by analogy with $K^0 \leftrightarrow \bar{K}^0$ mixing [11]. The parent atom virtually mixes, also with an amplitude of $\mathcal{O}(G_F^2)$, with the daughter one. Having two electron holes, the unstable daughter “leaks”. Consider the most general case including the possibility that the daughter nucleus be unstable and let $E \equiv E_H + E_{H'} + E^*$ and $\Gamma \equiv \Gamma_H + \Gamma_{H'} + \Gamma^*$. Let ΔM be the non-diagonal element of the mass matrix

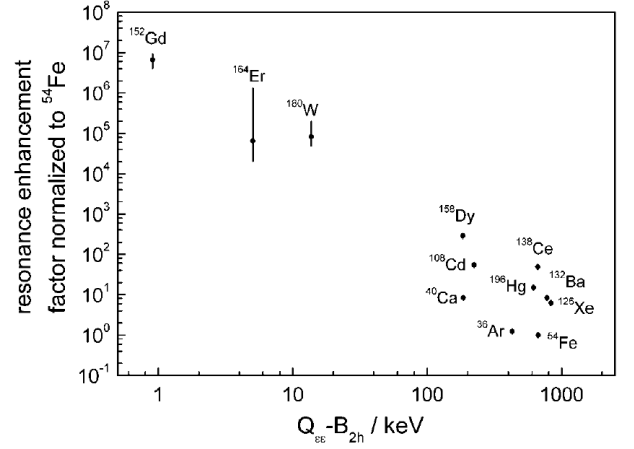


FIG. 16: Enhancement factors of no-neutrino DEC isotopes, relative to ^{54}Fe [21]. Notice the result for ^{152}Gd .

of the parent-daughter system. This suffices to write, for the lifetime τ and half-life $T_{1/2}$ of no-neutrino DEC:

$$\frac{1}{\tau} \equiv \frac{\ln 2}{T_{1/2}} = \frac{\Gamma}{(Q - E)^2 + \Gamma^2/4} (\Delta M)^2. \quad (17)$$

This expression transparently describes the name of the game: to find cases with $Q - E$ as small as possible and ΔM not suppressed by angular momentum conservation (i.e. not involving a forbidden nuclear transition).

The form of ΔM is simple, at least for the $^{112}\text{Sc} \rightarrow ^{112}\text{Cd}^*$, $0^+ \rightarrow 0^+$ transition to an excited nucleus with $E^* = 1.871$ MeV we favoured in [11], or the decay $^{152}\text{Gd} \rightarrow ^{152}\text{Sm}$, a $0^+ \rightarrow 0^+$ (ground state) case favoured after the precise Q -value determinations of [21]. To wit:

$$\Delta M = \frac{1}{4\pi R_N} (G_F \cos \theta_C)^2 \varphi_H(0) \varphi_{H'}(0) g_A^2 |\mathcal{M}| \bar{m}_\nu, \quad (18)$$

where $R_N = \langle R^2 \rangle^{1/2}$ is the root-mean-squared nuclear radius and $|\mathcal{M}|$ (a number) is the rest of the nuclear matrix element. The precise calculation of $|\mathcal{M}|$ is not simple, but ample progress has been recently made [36].

An up-to-date calculation of the neutrino-less half-life of ^{152}Gd [12, 38] results in:

$$T_{1/2} = 10^{26} |1 \text{ eV}/\bar{m}|^2 \text{ years}, \quad (19)$$

in the ballpark of the limits in searches for neutrino-less double β -decay. This opens up the possibility of using this isotope in a calorimetric experiment [12].

VII. THE SUM OF NEUTRINO MASSES

Cosmological observations place upper limits on $\sum m_\nu$, the sum of masses of three light neutrinos. These limits are quite model dependent and vary strongly with the data combination adopted, as illustrated in Fig. 17,

reproducing the recent Planck satellite results [39] for the normalized $\sum m_\nu$ probability distributions resulting from various combinations of input data and priors.

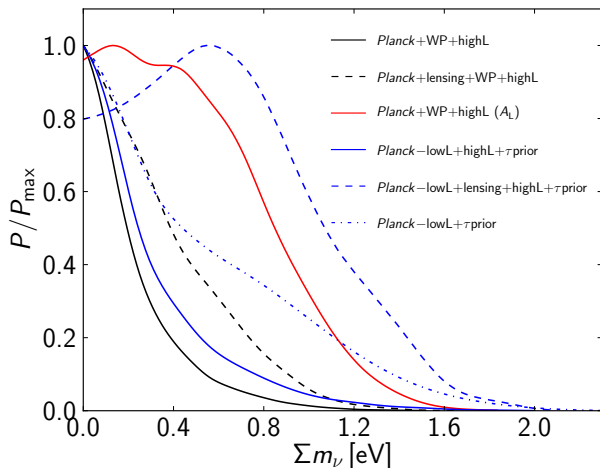


FIG. 17: The normalized $\sum m_\nu$ probability distributions and various combinations of data and priors. For details, see [39].

From their data, the Planck collaboration quotes 95% CL limits on $\sum m_\nu$ that range from 0.66 eV to 1.31 eV, depending on the chosen data and priors [39].

The neutrino oscillation data are not subject to the complications and subtleties of cosmological analyses. They provide *lower* limits on the sum of neutrino masses for three neutrino species:

$$\begin{aligned} \sum_i m_{\nu i} &> 0.06 \text{ eV}, \\ \sum m_{\nu i} &> 0.1 \text{ eV}, \end{aligned} \quad (20)$$

for a normal-hierarchy and for an inverted-hierarchy of masses, respectively [37]. These results do establish a target for direct-measurement experiments to aim at.

VIII. CONCLUSIONS

I have argued that the theory required to analyze the results of past and future calorimetric measurements of

the electron neutrino mass is simple and precise enough. This statement applies to single electron capture processes, as well as the neutrino-less double electron capture ones that are relevant only if neutrinos are Majorana.

The calorimetric measurements in the case of allowed nuclear transitions, that I have extensively discussed for EC in ^{163}Ho , should not have any of the atomic and molecular complications present in spectrometric β -decay experiments. The sophisticated calorimeters, thermometers, read-out electronics and source-preparation tools required for these experiments to be quantitatively competitive are being developed only recently, with decades of delay relative to β decay. But micro-calorimeters have the irresistible aesthetic advantage of being tiny contraptions to measure a tiny mass.

Enormously improved data on the Q -values relevant to neutrino-less double electron capture point to ^{152}Gd as the optimal source, for which calorimetric measurements ought to be possible and theoretically very clean.

The masses of neutrinos, their weak mixing angles, the flux of cosmic rays, the density and height of the atmosphere, the lifetimes of pions and muons, the inner temperature of the Sun, its radius and density profile, the size and density of the Earth, the parameters required for the Sun and nuclear reactors to function... have all been chosen by nature –just so– that we can measure the properties of neutrinos in Earth-based experiments.

Thus, there is ample reason to hope that the previous paragraph can be made extensive to laboratory measurements of the mass of the electron-neutrino and of the Dirac or Majorana character of these particles.

Acknowledgements

I am very indebted to Maurizio Lusignoli for our collaboration, his suggestions and his very careful reading of the manuscript.

-
- [1] F. Perrin, Comptes Rendus, 197 (1933) 1625.
 - [2] E. Fermi, Nature, Rejected; Nuov. Cim. 11 (1934) 1; Z. Phys. 88 (1934) 161.
 - [3] For a thorough recent review, see G. Drexlin et al. Advances in High Energy Physics (2013) ID 293986, <http://dx.doi.org/10.1555/2013/293986>.
 - [4] A. De Rújula, Nucl. Phys. **B188** (1981) 414
 - [5] A. De Rújula and M. Lusignoli, Phys. Lett. B118 (1982) 429
 - [6] W. Bambynek et al., Rev. Mod. Phys. 49 (1977) 77
 - [7] M. Sisti et al., Nuc. Instr. Methods, A520 (2004) 125; A. Nucciotti et al., Nuc. Instr. Methods, A520 (2004) 148; C. Arnaboldi et al., Phys. Rev. Lett. 91 (2003) 16802
 - [8] F. Gatti, Nuc. Phys. B91 (2001) 293
 - [9] W. H. Furry, Phys. Rev. 56 (1939); R. G. Winter, Phys. Rev. 100 (1955) 142
 - [10] H. M. Georgi, S. L. Glashow and S. Nussinov, Nuc. Phys. B193 (1981) 297

- [11] J. Bernabeu, A. De Rújula and C. Jarlskog, Nucl. Phys. B223 (1983) 15
- [12] S. A. Eliseev, Yu. N. Novikov and K. Blaum, J. Phys. G: Nuc. Part. Phys. 39 (2012) 124003
- [13] C. Kraus et al., Eur. Phys. J. C40 (2005) 447
- [14] Aseev et al., Phys. Rev. D84, 112003 (2011)
- [15] A full nuclear-structure calculation revises this result by a factor 0.962 ± 0.002 ; G.E. Brown and W. Weise, Phys. Rep. 22, 280 (1975).
- [16] R. Dvornicky et al., Phys. Rev. C 83 (2011) 045502
- [17] J. A. Formaggio, <http://arxiv.org/abs/1101.6077>
- [18] B. Monreal & J. A. Formaggio, Phys. Rev. D80 (2009) 051301
- [19] P. C.-O. Ranitzsch, J.-P. Porst, S. Kempf, et al., Jour. of Low Temp. Phys., 167, (2012) 1004
- [20] G. Audi, A. H. Wapstra, and C. Thibault, Nuc. Phys. A729 (2003) 337
- [21] K. Blaum, Phys. Rep. 425 (2006) 1. K. Blaum, Y. N. Novikov, and G. Werth, Contemporary Physics, 51 (2010) 149
- [22] C. L. Bennett, A. L. Hallin, R. A. Naumann et al., Phys. Lett. B107 (1981) 19
- [23] P. T. Springer, C. L. Bennett, and P. A. Baisden, Phys. Rev. A35 (1987) 679
- [24] R. J. Glauber and P. C. Martin, Phys. Rev. 104 (1956) 158; R. J. Glauber and P. C. Martin, Phys. Rev. 109 (1958) 1307
- [25] F. Gatti, P. Meunier, C. Salvo, and S. Vitale, Phys. Lett. B398 (1997) 415
- [26] S. Yasumi, M. Maezaba, K. Shima et al., Phys. Lett. B334 (1994) 229.
- [27] P. C.-O. Ranitzsch, J.-P. Porst, S. Kempf, et al., Journal of Low Temperature Physics 167 (2012) 1004
- [28] M. Lusignoli and M. Vignati, Phys. Lett. B697 (2011) 11
- [29] J. L. Campbell and T. Papp, Atomic Data and Nuclear Data Tables, 77 (2001) 1
- [30] I. M. Band and M. B. Trzhaskovskaya, Atomic Data and Nuclear Data Tables, 35 (1986) 1
- [31] E. J. McGuire, Phys. Rev. A5 (1972) 1043 and 1052; Phys. Rev. A9 (1974) 1840; Sandia Labs. Reps. SC-RR-71 0835, SAND-75-0043
- [32] A. De Rújula and M. Lusignoli, Nuc. Phys. B219 (1983) 277
- [33] A. D. MacLean and R. S. McLean, Atomic Data and Nuclear Data Tables 26 (1981) 197
- [34] L. Gastaldo, P. Ranitzsch, F. von Seggern et al., arXiv:1206.5647
- [35] I am indebted to M. W. Rabin for this warning.
- [36] M. Doi and T. Kotani, Prog. Theor. Phys., 89 (1993) 139; Z. Sujkowski and S. Wycech, Phys. Rev. C70 (2004) 052501; J. D. Vergados, Phys. Rev. C84 (2011) 044328; J.D. Vergados, H. Ejiri and F. Simkovic arXiv:1205.0649v2; D. Frekers arXiv:0506002; J. Vergados, 2002 Phys. Rep. 361 (2002) 1; F. Simkovic et al., Phys. Rev. C79 (2009) 055501; M. Krivoruchenko et al., 2011 Nucl. Phys. A859 (2012) 140; J. Suhonen, Phys. Lett. B701 (2011) 490
- [37] C. Gonzalez-Garcia et al., JHEP 1212 (2012) 123
- [38] D-L. Fang et al., Phys. Rev. C85 (2012) 035503; T. R. Rodríguez and G. Martínez-Pinedo, Phys. Rev. C85 (2012) 044310
- [39] Planck Collab.: P. A. R. Ade et al., arXiv:1303.5076